Axions, ALPs and other astroparticles in stellar interiors and the importance of precise nuclear reaction rates

Oscar Straniero
INAF-Teramo
INFN-Napoli -> LNGS
(LUNA collaboration)

LUNA (MV), o più in generale gli esperimenti di astrofisica nucleare, non producono (direttamente) risultati di “nuova fisica”, ma possono rendere felice un sacco di gente che cercano nuova fisica.

A promising case: Axion cooling in stellar interiors

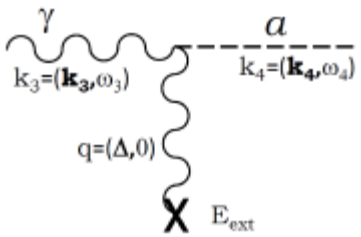

Primakoff

Based on http://arxiv.org/abs/1406.6053

The axion-photon Lagrangian is

$$\mathcal{L} = -\frac{g_{a\gamma}}{4} F\tilde{F} = g_{a\gamma}\mathbf{E}\cdot\mathbf{B} \qquad (1)$$

The electromagnetic field has a radial and an external component. So, $\mathbf{E} = \mathbf{E}_{\rm ext} + \mathbf{E}_{\rm rad}$ and $\mathbf{B} = \mathbf{B}_{\rm ext} + \mathbf{B}_{\rm rad}$. Of all the terms, we keep only

$$\mathcal{L} = g_{a\gamma}\mathbf{E}_{\rm ext}\cdot\mathbf{B}_{\rm rad} = g_{a\gamma}\mathbf{E}_{\rm ext}\cdot\nabla\times\mathbf{A}\,, \qquad (2)$$

$$g_{a\gamma} = 2\times 10^{-10}\ \ {\rm GeV}^{-1}\zeta\,({\rm m_a}/1\ {\rm eV})$$

ζ=1 in KSVZ model

Solar Axions Telescope at CERN

The predicted solar axion spectrum is currently searched by the CERN Axion Solar Telescope (CAST) [23], looking for conversions into X-rays of solar axions in a dipole magnet directed towards the sun. CAST searches with vacuum inside the magnet bores achieved a limit of $g_{a\gamma} \lesssim 0.88 \times 10^{-10}$ GeV^{-1} for $m_a \lesssim 0.02$ eV [23], an excellent constraint for very light ALPs. For realistic QCD axions, CAST has explored the mass range up to 1.17 eV, providing the bound $g_{a\gamma} \lesssim 2.3 - 3.3 \times 10^{-10}$ GeV^{-1} at 95 % CL, by using ^{4}He [24] and ^{3}He [25, 26] as buffer gas.

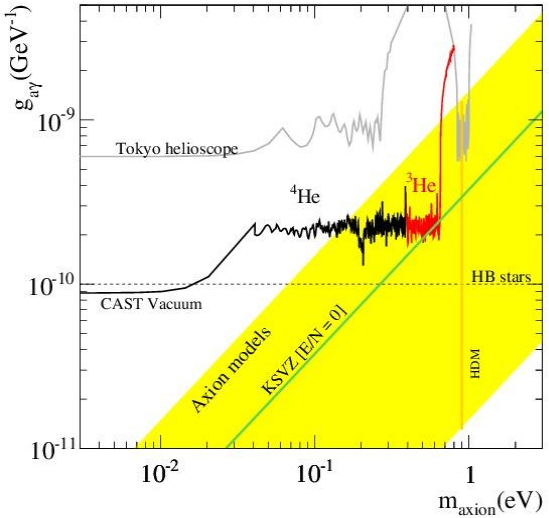

Scattering cross section

$$\sigma = \frac{1}{8\pi}\int_{-1}^{1}|\mathcal{M}|^2 dx = \frac{(Ze\,g_{a\gamma})^2}{16\pi}\int_{-1}^{1}\frac{|F(\mathbf{q})|^2}{q^4}\,|\mathbf{k}_4\times\mathbf{k}_3|^2\,dx. \tag{9}$$

To calculate the cross section, Eq. (9), we now use the following kinematic relations:

- $|\mathbf{k}_4| = \omega_4 = \omega_3$,
- $|\mathbf{k}_3| = \sqrt{\omega_3^2 - \omega_{\rm pl}^2}$,
- $|\mathbf{k}_4\times\mathbf{k}_3|^2 = |\mathbf{k}_4|^2|\mathbf{k}_3|^2\sin^2(\mathbf{k}_4,\mathbf{k}_3) = \omega_3^2\left(\omega_3^2-\omega_{\rm pl}^2\right)(1-x^2)$,
- $|\mathbf{q}|^2 = |\mathbf{k}_4-\mathbf{k}_3|^2 = |\mathbf{k}_4|^2+|\mathbf{k}_3|^2-2x|\mathbf{k}_4||\mathbf{k}_3| = 2\omega_3^2-\omega_{\rm pl}^2-2x\omega_3\sqrt{\omega_3^2-\omega_{\rm pl}^2}$,

$$F(\mathbf{q}) = \frac{\rho(\mathbf{q})}{Ze} = \frac{1}{Ze}\int\rho(x)e^{i\mathbf{q}\cdot\mathbf{x}}d\mathbf{x},$$

In these expressions[1], $\omega_{\rm pl}^2 = 4\pi\alpha n_e/m_e$ is the plasma frequency which changes the dispersion relations of the photon in a plasma.[2]

Non- degenerate electrons

$$\sigma = \frac{(Ze\,g_{a\gamma})^2}{64\pi}I(y,y_0,y_1) \tag{14}$$

$$I = \int_{-1}^{1}\frac{1-x^2}{(s+r-x)(r-x)}\,dx = \frac{r^2-1}{s}\ln\left(\frac{r-1}{r+1}\right)+\frac{(r+s)^2-1}{s}\ln\left(\frac{s+r+1}{s+r-1}\right)-2. \tag{15}$$

Energy loss rate

$$\varepsilon_{\rm nd} = \frac{n_t}{\rho\pi^2}\int_{\omega_{\rm pl}}^{\infty}\frac{\omega_3^2\sqrt{\omega_3^2-\omega_{\rm pl}^2}\,\sigma}{e^{\omega_3/T}-1}\,d\omega_3 = \frac{(Z^2n_t)g_{a\gamma}^2\alpha T^4}{16\rho\pi^2}\int_{y_0}^{\infty}\frac{y^2\sqrt{y^2-y_0^2}}{e^y-1}\,I\,dy\,,$$

Axions energy loss (erg/g/ s)

$$
\begin{cases}
\varepsilon_{\rm nd} = 7.1\times 10^{-52}\, g_{10}^2 \left(\frac{T^7}{\rho}\right) y_1^2\, f(y_0, y_1)\,, \\
\varepsilon_{\rm ions} = 7.1\times 10^{-52}\, g_{10}^2 \left(\frac{T^7}{\rho}\right) y_{\rm ions}^2\, f(y_0, y_{\rm ions})\,, \\
\varepsilon_{\rm el} = 4.7\times 10^{-31}\, g_{10}^2\, R_{\rm deg} \left(\frac{T^4}{\mu_e}\right) f(y_0, y_{\rm TF})\,, \\
\varepsilon_{\rm deg} = \varepsilon_{\rm ions} + \varepsilon_{\rm el}\,, \\
\varepsilon_{\rm Tot} = (1-w)\varepsilon_{\rm nd} + w\,\varepsilon_{\rm deg}\,.
\end{cases}
$$

$$
\begin{cases}
\zeta = \dfrac{3.01\times 10^5}{T}\left(\dfrac{\rho}{\mu_e}\right)^{2/3}\,, \\
w = \dfrac{1}{\pi}\arctan(\zeta - 3) + \frac{1}{2}\,.
\end{cases}
$$

$$
R_{\rm deg} \simeq \frac{1.5}{{\rm Max}(1.5, \zeta)}
$$

$$
f(y_0, y_*) = \frac{100}{1+y_*^2}\frac{1+y_0^2}{1+e^{y_0}}\, g(y_0, y_*)\,,
$$

$$
\begin{cases}
y_0 = \dfrac{3.33\times 10^5}{T}\dfrac{(\rho/\mu_e)^{1/2}}{(1+(1.019\times 10^{-6}\rho/\mu_e)^{2/3})^{1/4}}\,, \\
y_1 = 2.57\times 10^{10}\left[\dfrac{\sum_{\rm ions}(Z_j^2+Z_j)\,X_j}{A_j}\right]^{1/2}\left(\dfrac{\rho_0}{T_0^3}\right)^{1/2}\,, \\
y_{\rm ions} = \dfrac{\kappa_{\rm ions}}{T} = 2.57\times 10^{10}\left(\dfrac{\sum_{\rm ions} Z_j^2 X_j}{A_j}\right)^{1/2}\left(\dfrac{\rho}{T^3}\right)^{1/2}\,, \\
y_{\rm TF} = \dfrac{5.74\times 10^7}{T}\left(\dfrac{\rho}{\mu_e}\right)^{1/6}\,.
\end{cases}
$$

Axion e-loss rate, T_8=0.5, 1, 2

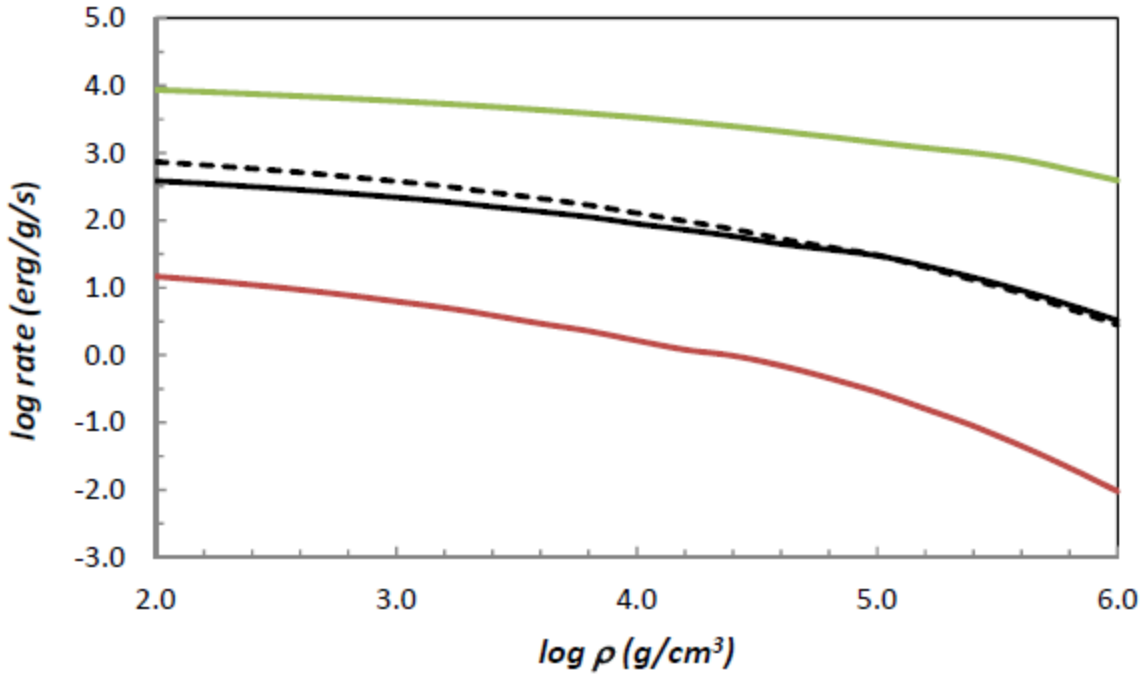

Fig. 2. Solid lines: axion production rate versus density for a pure He mixture and T= 5×10^7 K (red), 10^8 K (black) and 2×10^8 K (green). Dashed line: T= 10^8, but for pure C.

0.82 $M_\odot$: Just before the He-flash (RGB tip)

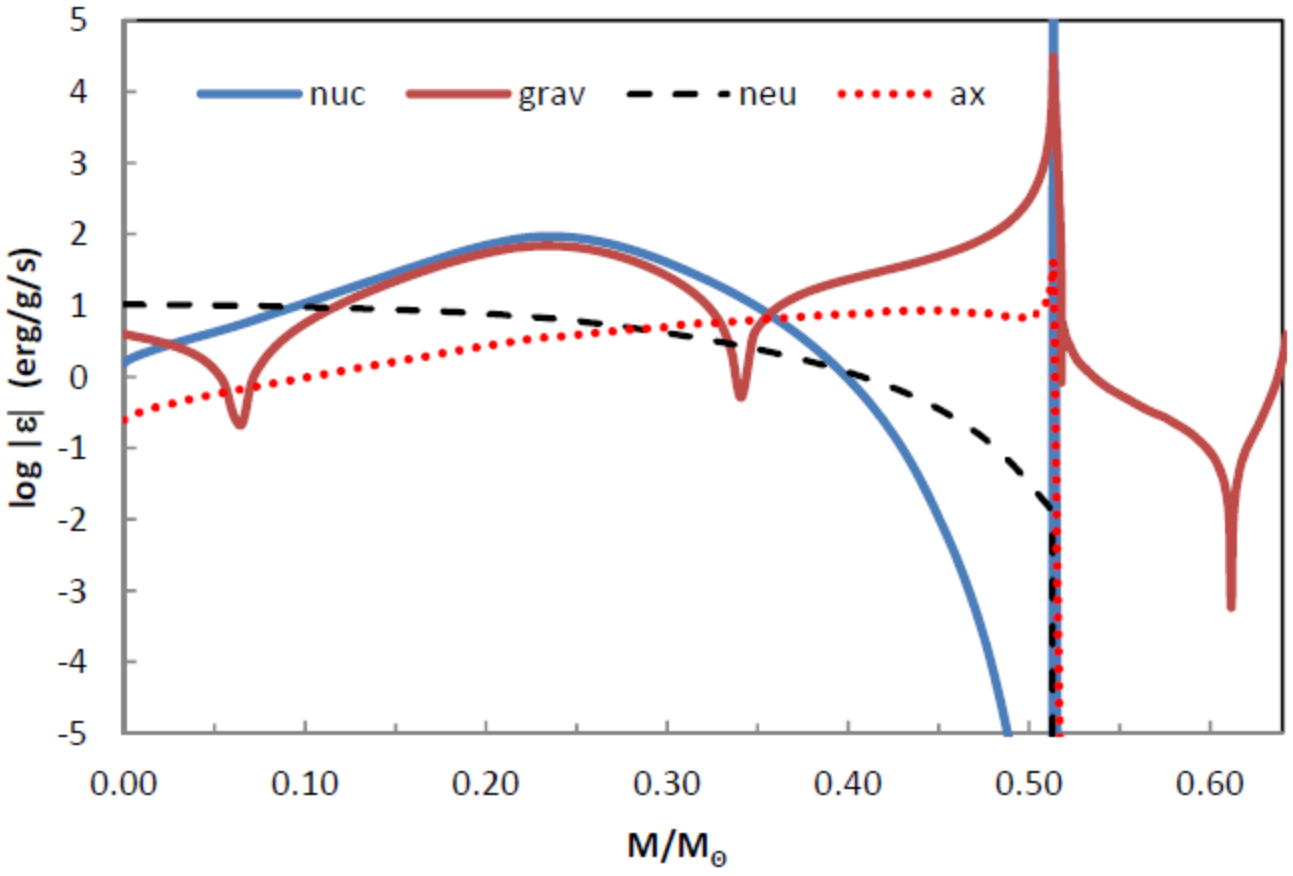

$g_{\alpha\gamma}=10^{-10}\ GeV^{-1}$

Core He burning (HB)

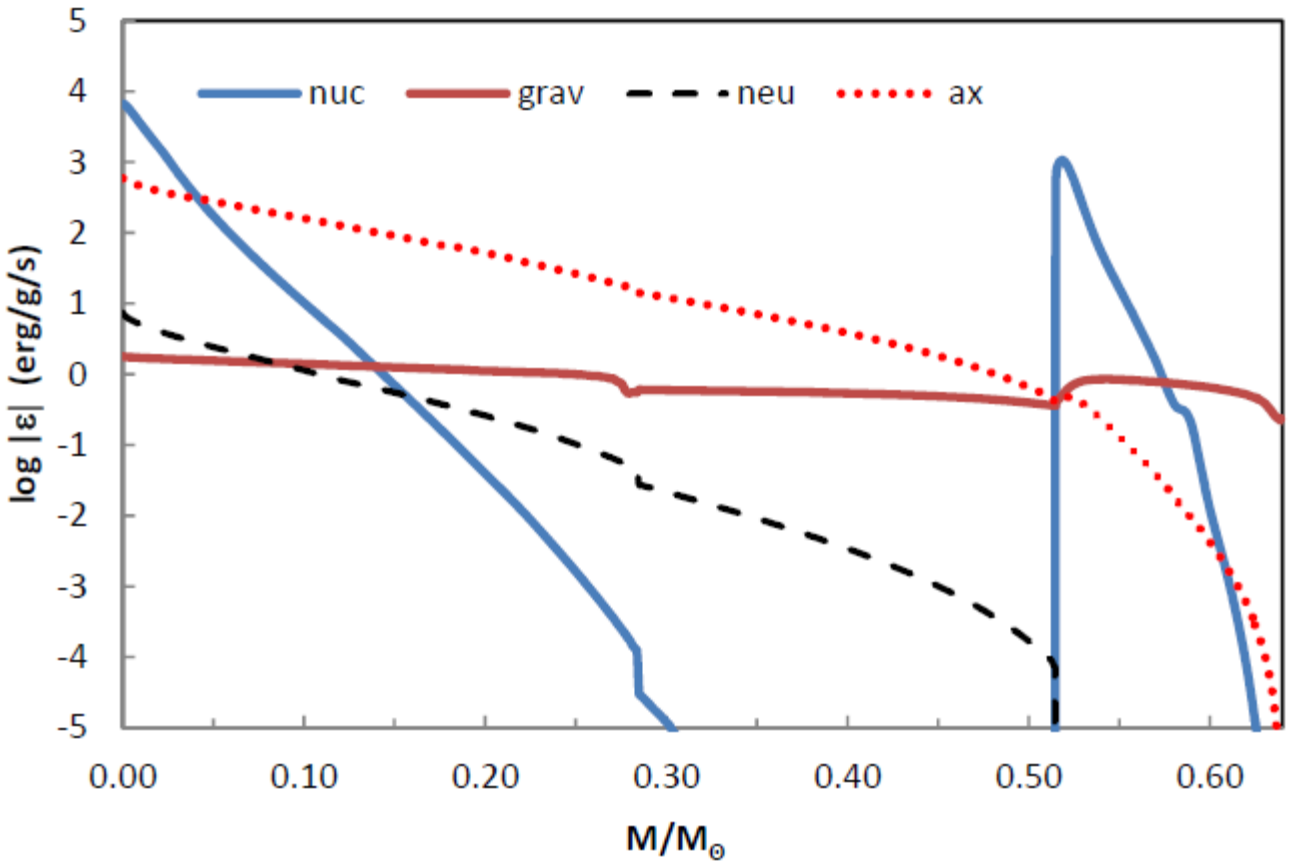

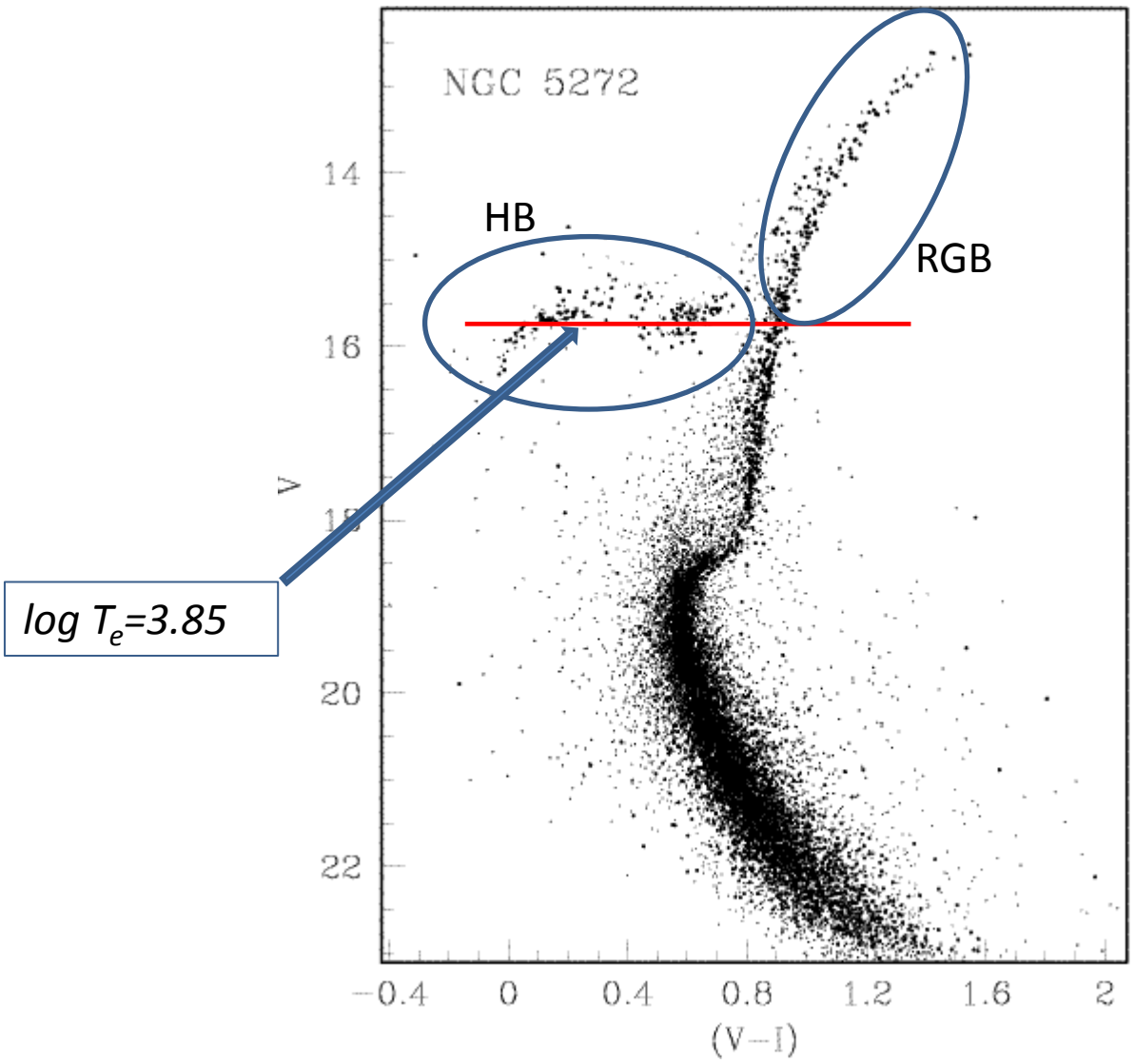

$$R = \frac{N_{HB}}{N_{RGB}}$$

39 Galactic Globular Clusters

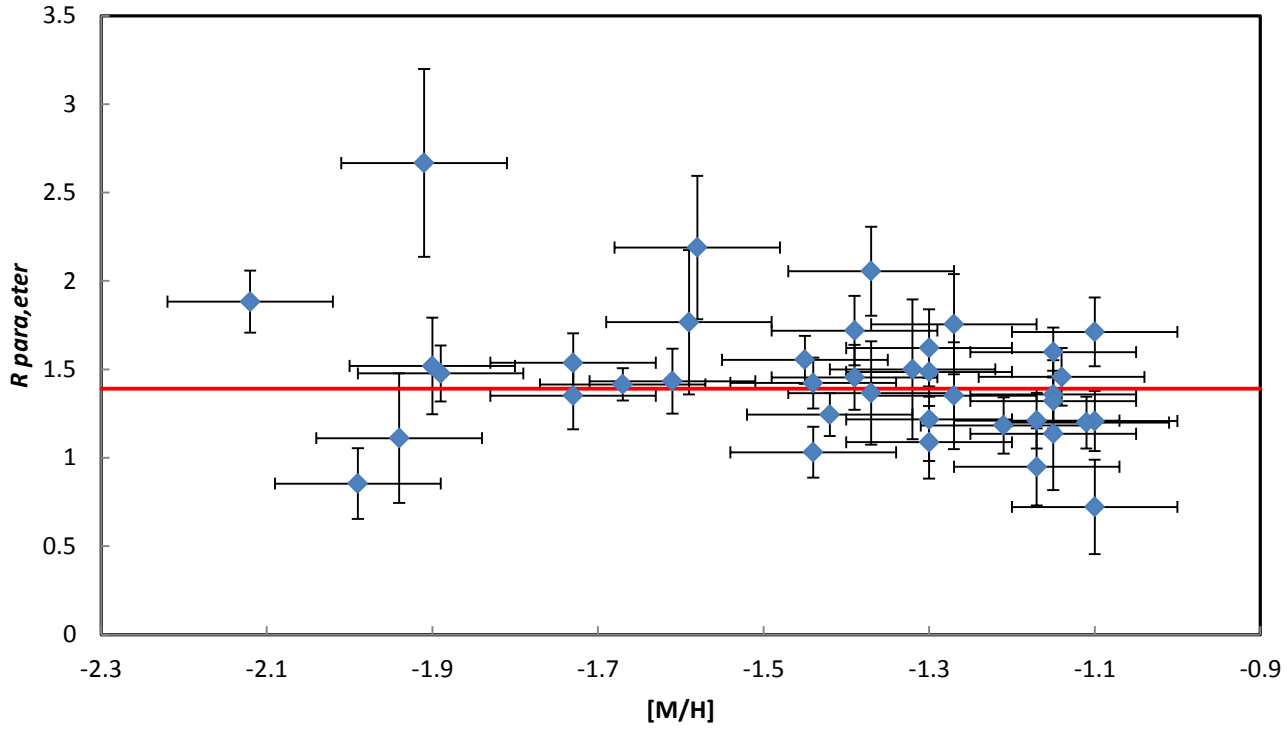

$\langle R_{GC} \rangle$ = 1.39±0.03 (68% CL)

$$R_{th}(g_{a\gamma}, Y) = 6.26 \times Y - 0.41 \times {g_{a\gamma}}^2 - 0.12$$

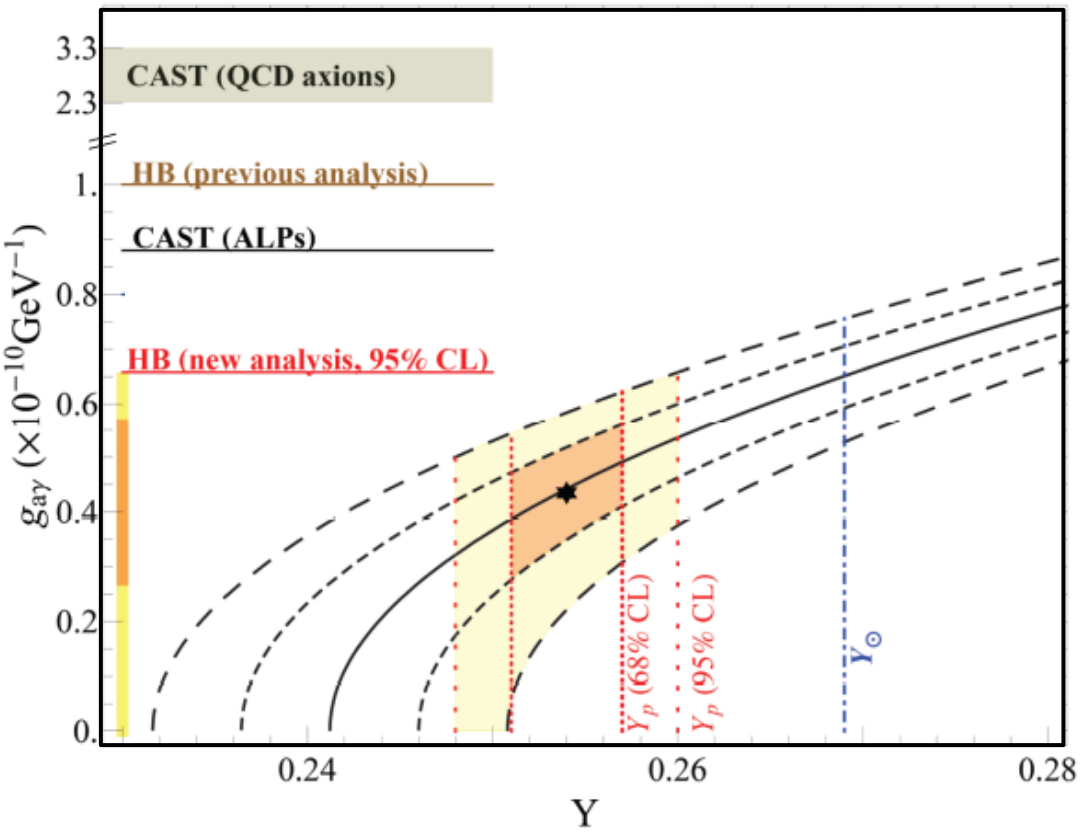

TABLE I: axion-photon coupling bounds

		R	Y	g_{10}
bounds from low-Z II regions	up 95%	1.33	0.260	0.66
-	up 68%	1.36	0.257	0.57
-	central value	1.39	0.254	0.45
-	low 68%	1.42	0.251	0.29
-	low 95%	1.45	0.248	0.00
bounds from SBBN	up 95%	1.33	0.2478	0.50
-	up 68%	1.36	0.2475	0.42
-	central value	1.39	0.2472	0.31
-	low 68%	1.42	0.2469	0.15
-	low 95%	1.45	0.2466	0.00
bounds from $Y_\odot$	up 95%	1.33	0.269	0.76
-	up 68%	1.36	0.269	0.71

$$g_{a\gamma} = 0.45^{+0.12}_{-0.16} \times 10^{-10}\ \mathrm{GeV}^{-1} \quad (68\%\ \mathrm{CL})\ ,$$

Ayala, Dominguez, Giannotti, Mirizzi & Straniero 2014, PRL accepted

Y from low-Z HII extragalactic region

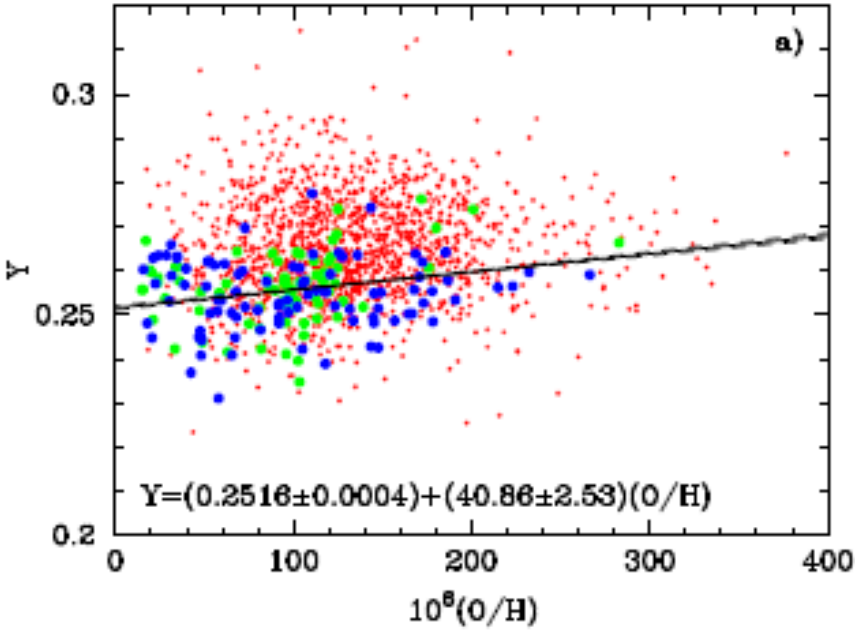

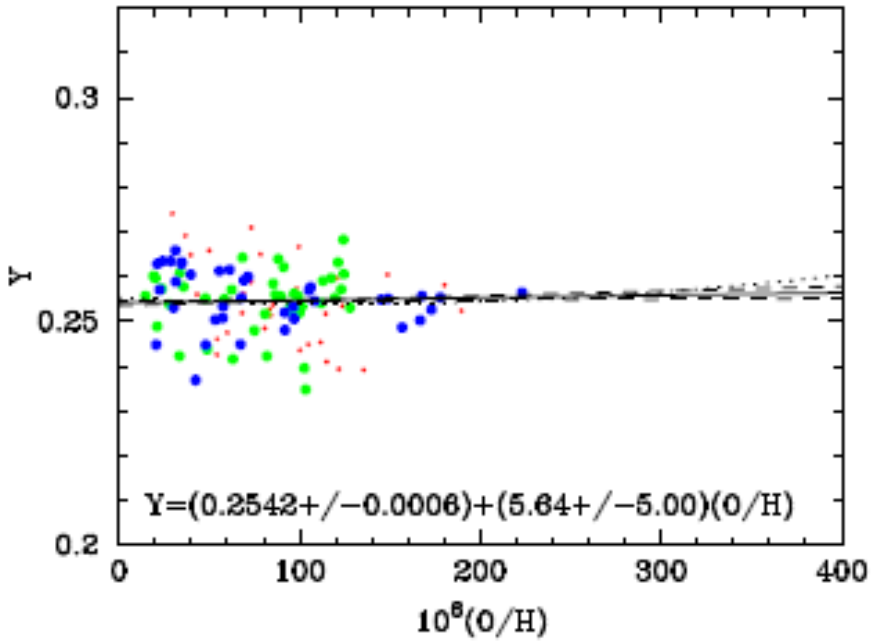

Izotov et al. 2013

Axion cooling competes with the nuclear energy production

Gamow's peak energy

$$E_0 = \left(\frac{bKT}{2} \right)^{1/2}$$

T = 70 MK (RGB)	
14N+p	65 KeV
T = 200 MK (He-burning)	
12C+α	300 KeV
T = 500 MK (C-burning)	
12C+12C	1.5 MeV

- $^{14}N(p,\gamma)^{15}O$ LUNA400 (LUNA MV)
- 3a (?)
- $^{12}C(\alpha,\gamma)^{16}O$ main target LUNA MV
- $^{12}C(^{2}C,\gamma)^{24}Mg^{*}$ LUNA MV ?

$^{14}N(p,\gamma)^{15}O$ the bottleneck of CNO

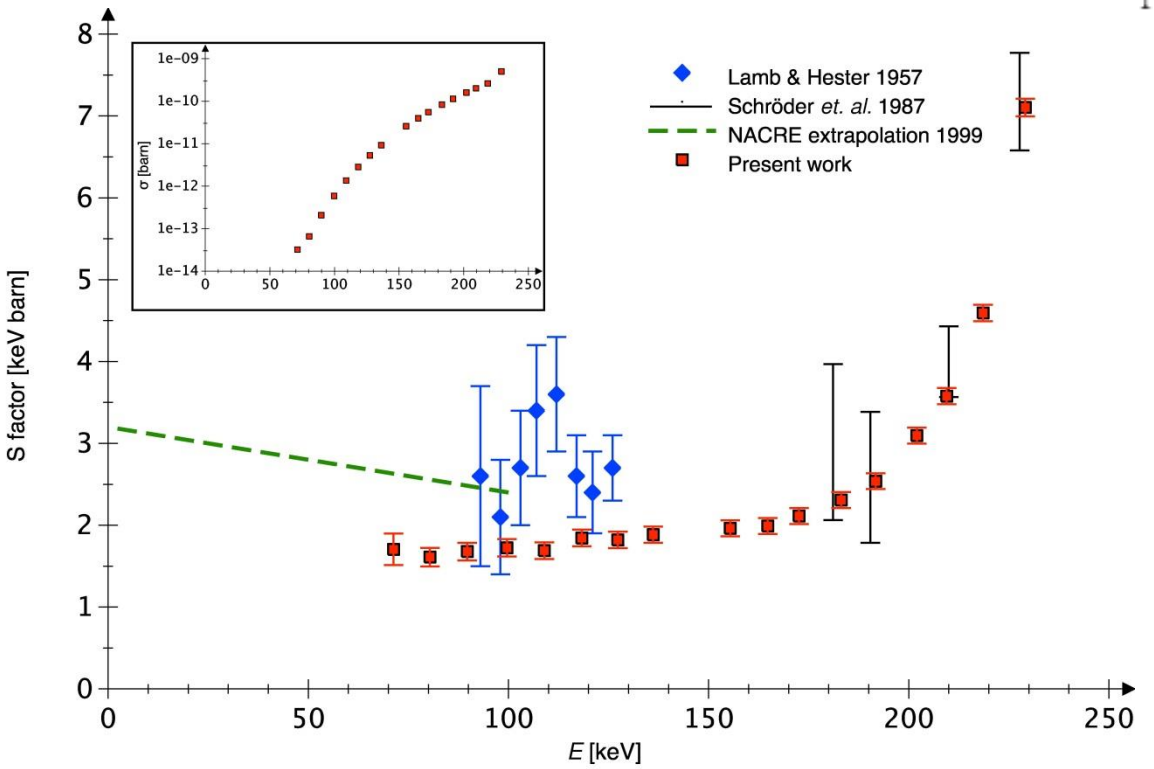

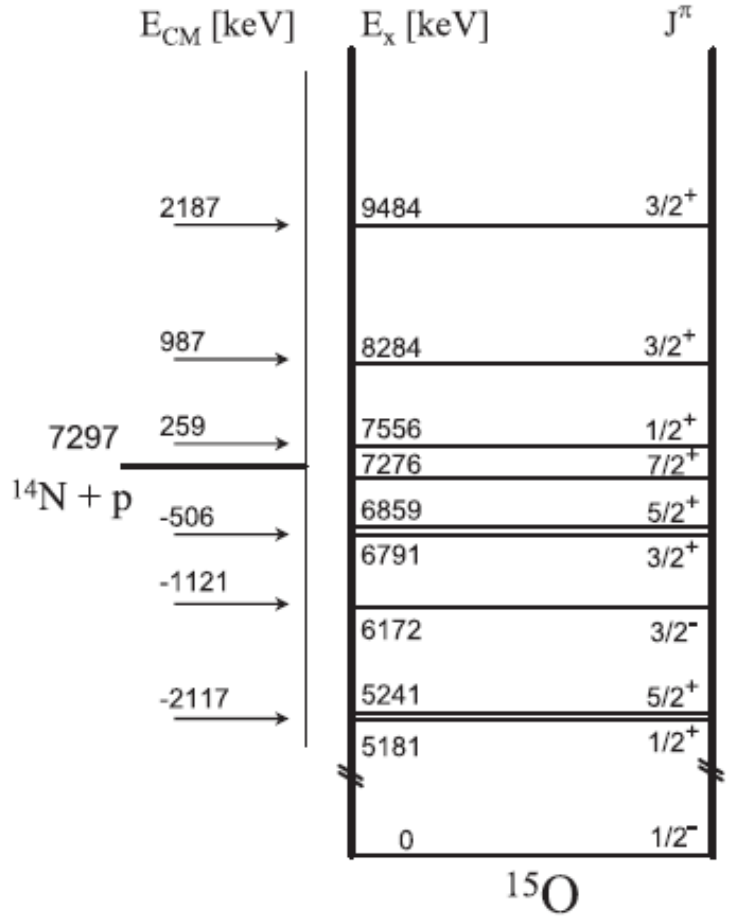

LUNA

Formicola et al. 2005

Imbriani et al. 2005

From Adelberger et al. 2011

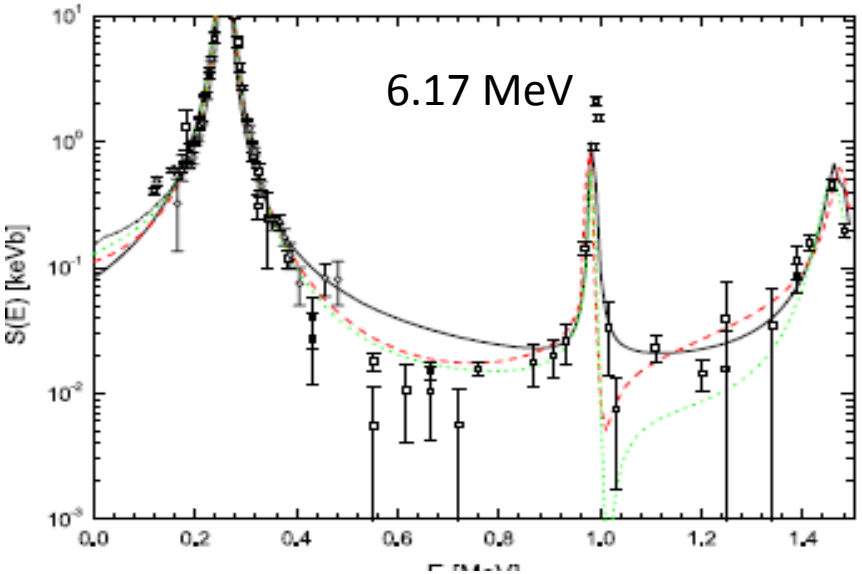

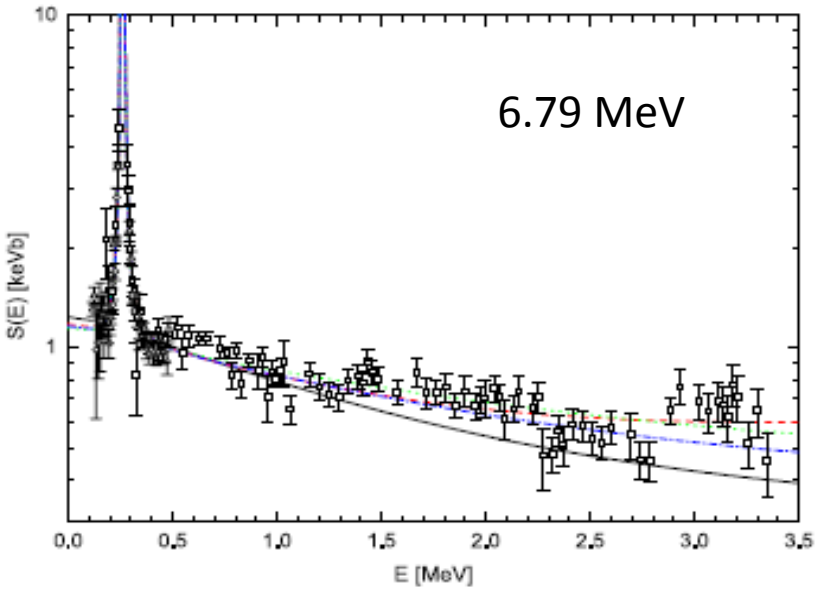

A unique setup for a large range of E: possible with LUNA MV

$N_a\langle\sigma,v\rangle$ (10^{-15} $cm^3 mol^{-1} s^{-1}$) for T_9=0.2

	Low	Adop.	high
Kunz et al 2001	5.25	7.58	10.2
Buchmann 1996	3.04	7.04	13.04
NACRE	5.44	9.11	12.8
CF88		4.74	
CF85		11.3	

Not an error bar

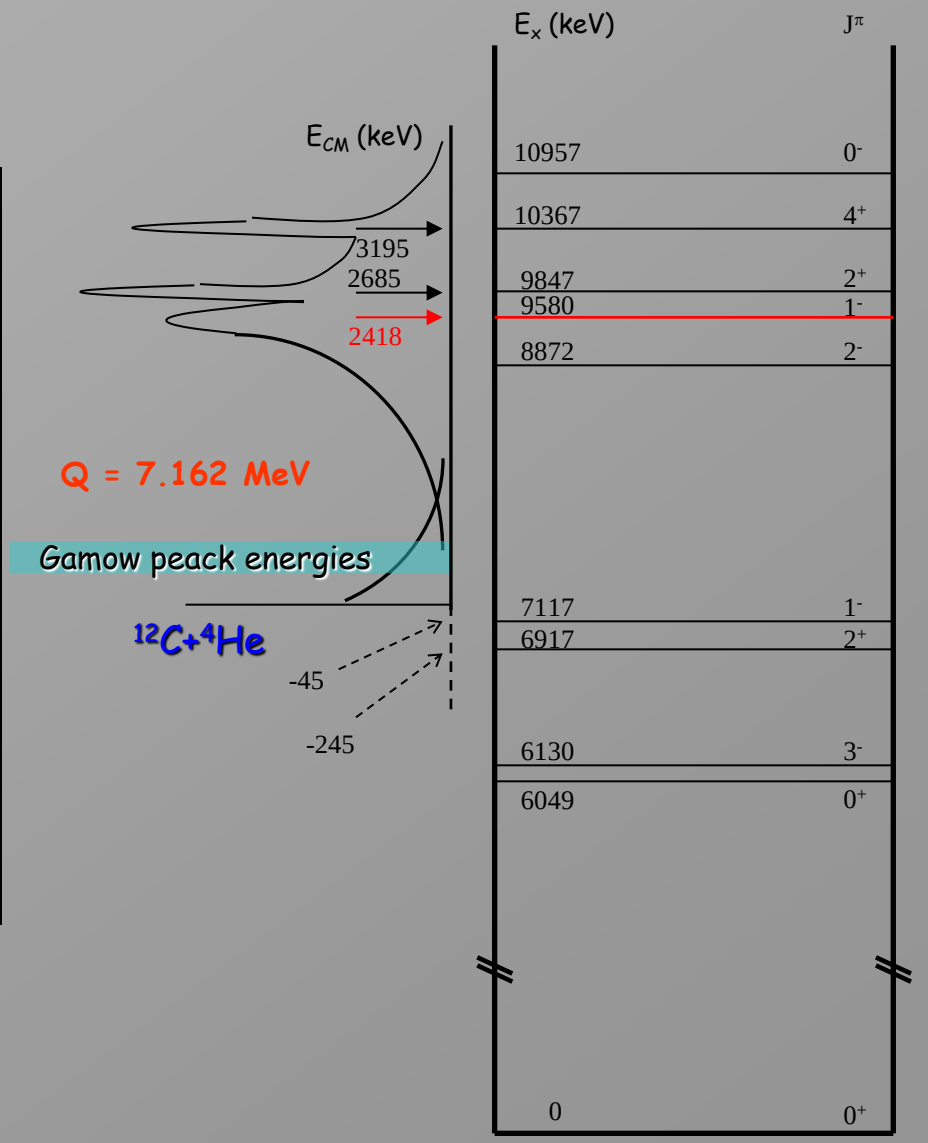

16O level scheme

$^{12}C(\alpha,\gamma)^{16}O$

At the Gamow peak around E ~ 300 keV the cross section is dominated by ground state capture proceeding through two subthreshold resonances with $J^{\pi} = 1^{-}$ and 2^{+}. Those interfere with contributions from higher lying states and the direct capture process. In addition cascade transitions take place. The current estimates of the astrophysical cross section are based on R-Matrix analyses, taking into account direct measurements at higher energies (E > 1 MeV), elastic scattering data and the β–delayed α-spectrum of ^{16}N (providing information on the reduced width of the subthreshold 1^{-} state).

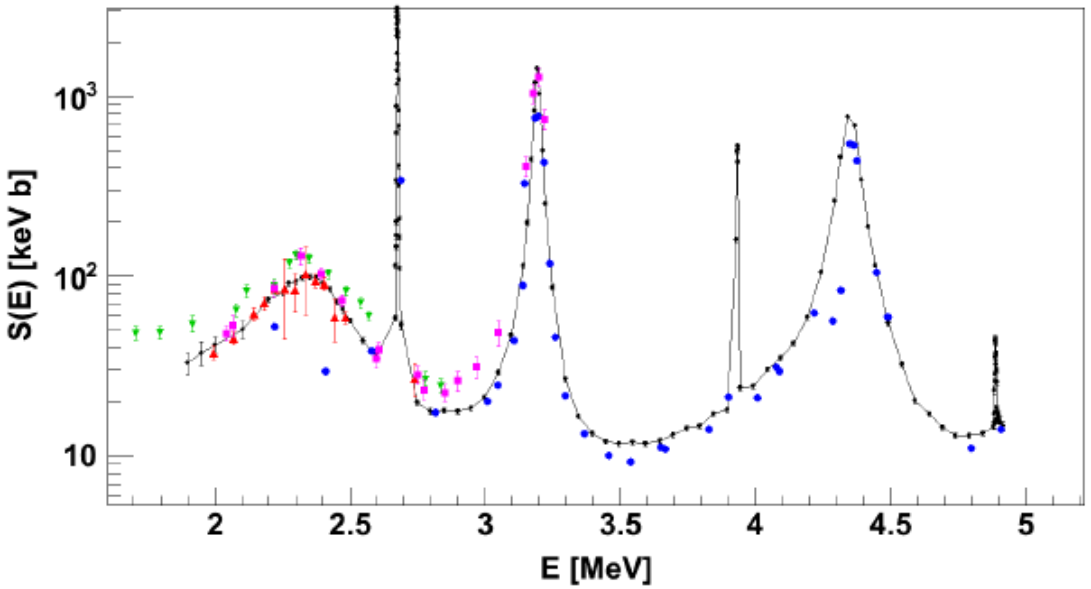

Figure 6 $^{12}C(\alpha,\gamma)^{16}O$ total cross section as measured by the RMS experiments ERNA (black dots with line to guide the eye, [5]) and DRAGON (solid blue circles, [21]) compared to the sum of all γ-ray transitions from the measurements of Kunz et al. (solid red triangles-up, [24][25]), Kettner et al. (solid magenta squares, [23]) and Redder et al. (solid green triangles-down, [22]). Good agreement is found between between ERNA and Kunz et al., while the DRAGON data points show larger deviations around the resonances at 2.4 and 4.4 MeV.